


# Vascular Response to Spreading Depolarization Predicts Stroke Outcome

**Journal Article****Author(s):**

Binder, Nadine Felizitas; Glück, Chaim; Middleham, William; Alasoadura, Michael; Pranculeviciute, Nikolette; [Wyss, Matthias](#) ; Chuquet, Julien; Weber, Bruno; Wegener, Susanne; El Amki, Mohamad

**Publication date:**

2022-04

**Permanent link:**

<https://doi.org/10.3929/ethz-b-000541593>

**Rights / license:**

[Creative Commons Attribution-NonCommercial-NoDerivatives 4.0 International](#)

**Originally published in:**

Stroke 53(4), <https://doi.org/10.1161/STROKEAHA.121.038085>



# Vascular Response to Spreading Depolarization Predicts Stroke Outcome

Nadine Felizitas Binder<sup>1</sup> PhD; Chaim Glück<sup>1</sup> PhD; William Middleham<sup>1</sup> MSc; Michael Alasoadura<sup>1</sup> MSc; Nikoleta Pranculeviute<sup>1</sup> MSc; Matthias Tasso Wyss<sup>1</sup> MD, PhD; Julien Chuquet<sup>1</sup> PhD; Bruno Weber, PhD; Susanne Wegener<sup>1</sup> MD\*; Mohamad El Amki<sup>1</sup> PhD\*

**BACKGROUND:** Cortical spreading depolarization (CSD) is a massive neuro-glial depolarization wave, which propagates across the cerebral cortex. In stroke, CSD is a necessary and ubiquitous mechanism for the development of neuronal lesions that initiates in the ischemic core and propagates through the penumbra extending the tissue injury. Although CSD propagation induces dramatic changes in cerebral blood flow, the vascular responses in different ischemic regions and their consequences on reperfusion and recovery remain to be defined.

**METHODS:** Ischemia was performed using the thrombin model of stroke and reperfusion was induced by r-tPA (recombinant tissue-type plasminogen activator) administration in mice. We used in vivo electrophysiology and laser speckle contrast imaging simultaneously to assess both electrophysiological and hemodynamic characteristics of CSD after ischemia onset. Neurological deficits were assessed on day 1, 3, and 7. Furthermore, infarct sizes were quantified using 2,3,5-triphenyltetrazolium chloride on day 7.

**RESULTS:** After ischemia, CSDs were evidenced by the characteristic propagating DC shift extending far beyond the ischemic area. On the vascular level, we observed 2 types of responses: some mice showed spreading hyperemia confined to the penumbra area (penumbral spreading hyperemia) while other showed spreading hyperemia propagating in the full hemisphere (full hemisphere spreading hyperemia). Penumbral spreading hyperemia was associated with severe stroke-induced damage, while full hemisphere spreading hyperemia indicated beneficial infarct outcome and potential viability of the infarct core. In all animals, thrombolysis with r-tPA modified the shape of the vascular response to CSD and reduced lesion volume.

**CONCLUSIONS:** Our results show that different types of spreading hyperemia occur spontaneously after the onset of ischemia. Depending on their shape and distribution, they predict severity of injury and outcome. Furthermore, our data show that modulating the hemodynamic response to CSD may be a promising therapeutic strategy to attenuate stroke outcome.

**GRAPHIC ABSTRACT:** A graphic abstract is available for this article.

**Key Words:** cortical spreading depolarization ■ hemodynamics ■ ischemic stroke ■ reperfusion ■ spreading hyperemia ■ thrombin

Cortical spreading depolarization (CSDs) are an initial mass depolarization of neurons and glial cells; subsequently followed by suppression of electrical activity that propagate through the cortex.<sup>1–3</sup> The onset of persistent depolarization triggers the breakdown of ion homeostasis and development of cytotoxic edema.<sup>4,5</sup> In patients with ischemic stroke as well as in

experimental models of stroke, CSDs define the ischemic core of an infarct and progress outward across the penumbra area.<sup>6,7</sup> There are different patterns of depression (silencing) that may be associated with spreading depolarization. Energy state and spontaneous activity of the tissue determines both (1) the duration of the spreading depolarization and (2) the depression pattern

Correspondence to: Mohamad El Amki, PhD, Department of Neurology, University Hospital Zurich, Frauenklinikstrasse 26, 8091 Zurich, Switzerland. Email mohamad.elamki@usz.ch

\*S. Wegener and M. El Amki are joint authors.

Supplemental Material is available at <https://www.ahajournals.org/doi/suppl/10.1161/STROKEAHA.121.038085>.

For Sources of Funding and Disclosures, see page 1394.

© 2022 The Authors. *Stroke* is published on behalf of the American Heart Association, Inc., by Wolters Kluwer Health, Inc. This is an open access article under the terms of the [Creative Commons Attribution Non-Commercial-NoDerivs](https://creativecommons.org/licenses/by-nc-nd/4.0/) License, which permits use, distribution, and reproduction in any medium, provided that the original work is properly cited, the use is noncommercial, and no modifications or adaptations are made.

*Stroke* is available at [www.ahajournals.org/journal/str](http://www.ahajournals.org/journal/str)

## Nonstandard Abbreviations and Acronyms

<b>CBF</b>	cerebral blood flow
<b>CSD</b>	cortical spreading depolarization
<b>DC</b>	direct current
<b>FHSH</b>	full hemisphere spreading hyperemia
<b>LSCI</b>	laser speckle contrast imaging
<b>MCA</b>	middle cerebral artery
<b>PSH</b>	penumbral spreading hyperemia
<b>ROI</b>	regions of interest
<b>r-tPA</b>	recombinant tissue-type plasminogen activator
<b>SH</b>	spreading hyperemia

that accompanies the depolarization. The 2 major types of silencing of spontaneous activity which can co-occur with spreading depolarization in stroke are nonspreading depression and spreading depression of spontaneous activity.<sup>4,5,8</sup>

From a hemodynamic point of view, spreading depolarizations are associated with dramatic changes in cerebral blood flow (CBF). CSDs evoke either transient hyperemia; or hypoperfusion (inverse hemodynamic response) depending on the metabolic condition of the tissue and the intactness of the neurovascular machinery.<sup>8</sup> Indeed, CSDs are typically accompanied by a transient spreading hyperemia (SH) in normal tissue. SHs provide oxygen and glucose to ischemic tissue, ultimately supporting the restoration of ionic equilibrium.<sup>4,9</sup> However, CSD propagation in ischemic tissue can cause vasoconstriction within the cortical microcirculation, leading to a transient hypoperfusion and accentuation of damage.<sup>10</sup> In rodents, the spreading depolarization extreme in ischemic tissue is characterized by prolonged depolarization durations, in addition to a slow baseline variation termed the negative ultraslow potential.<sup>11</sup> The more inverted the hemodynamic responses to spreading depolarization, the more critical the situation becomes for the tissue.<sup>12,13</sup> In addition to the negative ultraslow potential and the spreading depolarizations duration, studies in rodents have shown that a high number of CSDs results in larger ischemic brain lesions.<sup>2,8,14,15</sup> CSDs are not only indicators of severe brain injury, but they are the mechanism underlying the cytotoxic neuronal edema.<sup>7,16–18</sup> Furthermore, in patients with malignant middle cerebral artery (MCA) infarction, the prevalence of CSDs, assessed with subdural electrodes, can be higher than 75%, and patients with more CSDs had an even more detrimental outcome.<sup>19</sup> Importantly, even when recorded with a delay of several days, spreading depolarization occurred spontaneously with high frequency in stroke patients.<sup>7,20</sup>

Overall, the hemodynamic responses to CSD are heterogeneous, which brings up the question of their relation to the severity of tissue injury. Our goal was to study

the propagation profiles of SHs in mice subjected to ischemic stroke and reperfusion treatment by using wide field laser speckle contrast imaging (LSCI). We present a comprehensive analysis of the spatiotemporal propagation of SH postischemia, which we found to be strongly dependent on stroke severity.

## METHODS

The authors declare that upon request all supporting data are available within the article and its [Supplemental Material](#).

### Ethics and Animals

All animal experiments were approved by the local veterinary authorities in Zurich as well as the ethics committee for animal research of Normandy and the French ministry of higher education, research, and innovation. Experiments were conformed to the guidelines of the Swiss Animal Protection Law, Veterinary Office, Canton of Zurich (Act of Animal Protection December 16, 2005 and Animal Protection Ordinance April 23, 2008, animal welfare assurance number ZH165/19 and ZH224/15) and the European Community Council Directive 2010/63/UE of September 22, 2010 on the protection of animals used for scientific purposes. Experiments were performed on both male and female Balb/C mice (Charles Rivers, no.028), 10 to 12 weeks of age, weighting between 20 and 30 g. The mice were housed under standard conditions including free access to water and food as well as an inverted 12-hour light/dark cycle. A total of 51 adult mice were used in this study.

### Thrombin Stroke Model

For ischemic stroke induction, mice were anesthetized with a mixture of fentanyl (0.05 mg/kg bodyweight; Sintenyl, Sintetica), midazolam (5 mg/kg bodyweight; Dormicum, Roche), and medetomidine (0.5 mg/kg bodyweight; Domitor, Orion Pharma), which was injected intraperitoneally. During all procedures, the core temperature of the animals was kept constant at 37°C, using a homothermic blanket heating system (Harvard Apparatus).

We induced stroke using the thrombin model as described previously.<sup>21,22</sup> Briefly, a glass pipette was introduced into the lumen of the MCA and 1  $\mu$ L of thrombin (1UI; HCT-0020, Haematologic Technologies Inc) was injected to induce the formation of a clot in situ (Figure 1).

Ischemia induction was considered to be stable when CBF dropped to at least 50% of baseline level in MCA territory<sup>23</sup> and remained below 50% for at least 30 minutes. Sham-operated mice underwent the same surgical procedure without pipette insertion.

### In Vivo Electrophysiology

Two small holes were drilled in the parietal bone, and the dura-matter was incised with care to leave the cortex intact. Glass electrodes were filled with artificial CSF containing the following: 125 mmol/L NaCl, 2 mmol/L KCl, 1.3 mmol/L NaH<sub>2</sub>PO<sub>4</sub>, 26 mmol/L NaCO<sub>3</sub>, 10 mmol/L glucose, 2 mmol/L CaCl<sub>2</sub>, and 1 mmol/L MgSO<sub>4</sub>. Just after MCA occlusion, the electrodes were lowered into the cortex at a depth of 300  $\mu$ m to

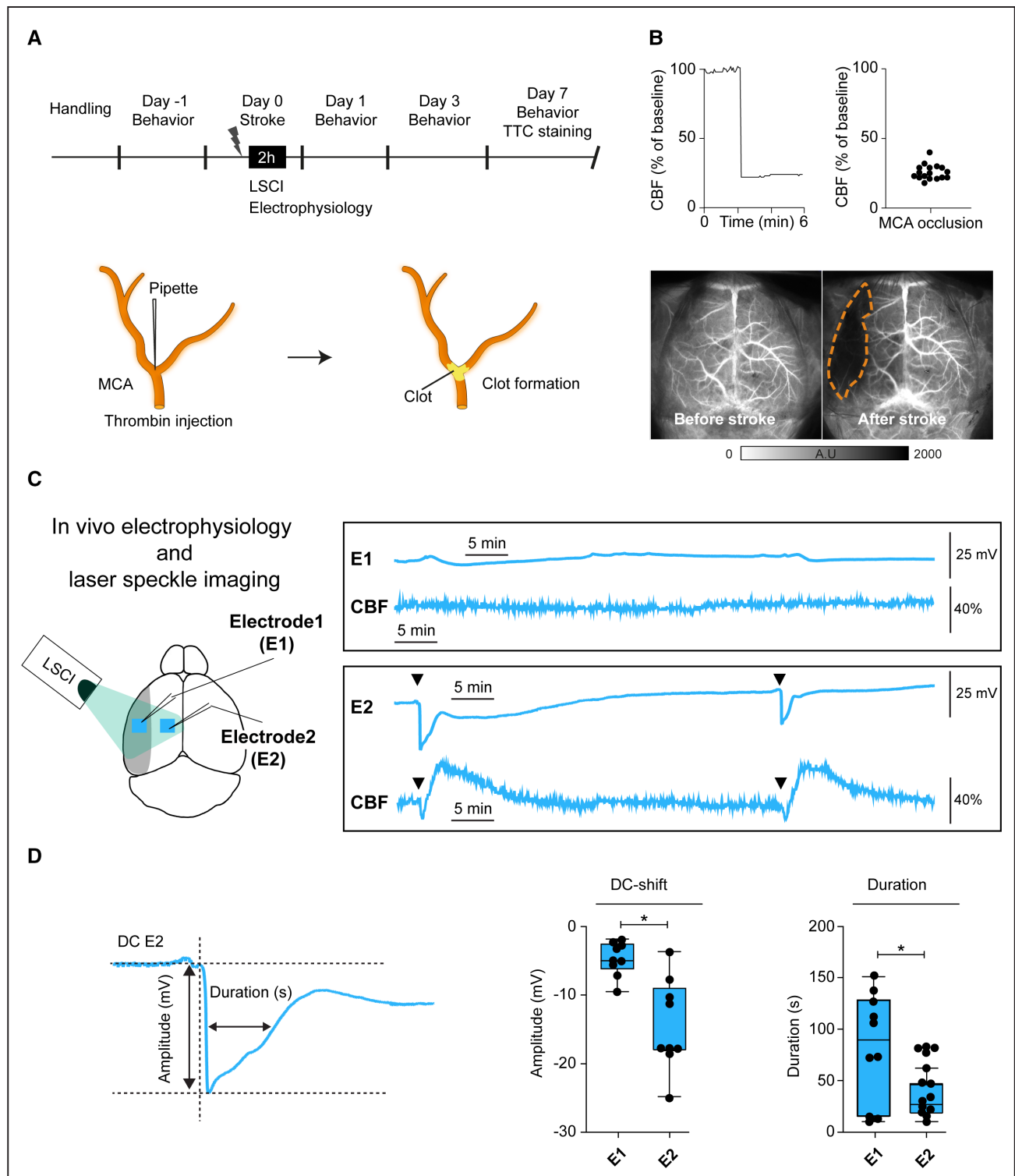


**Figure 1. Overview of experiments.**

**A**, Timeline of experiments. Sensorimotor tests were performed before stroke and on day 1, 3, and 7 poststroke. Cerebral blood flow (CBF) was recorded for 2 h after middle cerebral artery (MCA) occlusion by laser speckle contrast imaging (LSCI). Animals were euthanized after 7 days and brains extracted and stained with 2,3,5-triphenyltetrazolium chloride (TTC). In the **lower** part, schematic view of thrombin injection into the MCA-M2 segment. **B**, LSCI recordings in mice with ischemia. On the **left**: representative example of a single mouse, on the **right**: mean CBF drop after MCA occlusion ( $n=18$  mice). **Lower** part shows representative LSCI images of cortical perfusion before and after MCA occlusion. The color bar indicates perfusion in arbitrary units (A.U.). **C**, In vivo electrophysiology and LSCI recordings in a mouse showing spreading depolarization after ischemia. **D**, The amplitude of direct current (DC)-shift in the CSDs of the penumbra is higher than that of the core while the duration of the waves is shorter ( $n=6$  animals,  $*P < 0.05$ ; Mann-Whitney  $U$  test).

perform direct current (DC) coupled recordings. One electrode was placed in the core of the ischemic hemisphere, and the other electrode was placed in the penumbra region. A reference Ag/AgCl electrode was inserted superficially in the neck muscle. DC were amplified (DAM60; World Precision Instruments, Sarasota, FL), digitized at 20 kHz (Powerlab 8/35, AD Instruments, Australia) and recorded during 2 hours. The DC signals were analyzed with Labchart 8, (AD Instruments, Australia) software following the recommendations of the Co-Operative Study on Brain Injury Depolarizations group.<sup>24</sup>

In brief, the slow extracellular potential shifts of CSD were assessed after the low pass filter was set at 5 Hz. The DC-potential signals were amplified 100X (MultiClamp 700A, Molecular Devices) and low-pass filtered at 5 Hz.

### Laser Speckle Contrast Imaging

CBF was monitored using LSCI (FLPI, Moor Instruments, United Kingdom). Two regions of interest (ROI, 25×250 μm) were defined: the infarct core (ROI1) and the penumbra area (ROI2) as shown in Figure 2A and 2B. The penumbra region was defined as the area at risk surrounding the core, expanding to lesion in absence of reperfusion and showing microvascular alteration as described previously.<sup>21</sup> While the core region was within the MCA territory, the penumbra area was in the watershed zone and ACA territory of the infarcted hemisphere. The CBF drop in the core region (MCA territory) was defined as <50% of baseline as a threshold of cerebral ischemia, below which there is a progressive reduction in protein synthesis, which leads to an impaired neuronal activity and neurological deficits in rodents.<sup>21,25</sup> Therefore, this value was used as a threshold for exclusion of ischemic animals in several ischemic mouse models suggesting that these mice could have differences in severity of ischemia.<sup>26,27</sup>

### r-tPA Administration

Thirty minutes after induction of ischemia, thrombolysis was initiated via tail vein (200 μL, 1 mg/mL in 0.9% saline) of human r-tPA (recombinant tissue-type plasminogen activator; 10 mg/kg, Actilyse, Boehringer Ingelheim) according to previous studies.<sup>21,22</sup> Control groups received saline instead of r-tPA.

### Behavioral Assessment

Sensorimotor function was assessed by an investigator blinded to treatment before and after stroke on days 1, 3, and 7. Neurological deficits were obtained using a composite observational neurological score as well as the adhesive tape removal test as described previously.<sup>21,25</sup>

The neurological score is a composite grading score. For the adhesive tape removal test, 2 adhesive tape strips (rectangular 0.3×0.4 cm) were applied on both forepaws of each animal. The time the mouse took to contact (sensory function) and remove (motor function) the tapes on both paws were recorded. Before stroke, animals were trained to remove both adhesive tapes within 10 seconds.<sup>28,29</sup>

### Lesion Volume and Hemorrhage Assessment

Mice were euthanized by an overdose of pentobarbital (200 mg/kg, intraperitoneally). Brains were extracted and sliced into

1 mm thick coronal sections from 6.5 to 0.5 mm anterior to the interaural line. To determine infarct volume, slices were placed in 2% 2,3,5-triphenyltetrazolium chloride (catalog No. T8877, Sigma-Aldrich, St Louis, MO) for 10 minutes at 37 °C. A blinded investigator determined infarct areas using an image analysis system (Image J version 1.41). To correct for brain swelling, each infarct area was multiplied by the ratio of the surface of the intact (contralateral) hemisphere to the infarcted (ipsilateral) hemisphere at the same level. Total volume of damaged tissue, expressed as cubic millimeters, was calculated by linear integration of the corrected lesion areas.<sup>23</sup> The presence of hemorrhages was recorded by using 2,3,5-triphenyltetrazolium chloride stained slices at the time of premature death or after euthanasia at day 7.<sup>30</sup>

### Statistical Analysis

Statistical analysis was performed using GraphPad Prism (version 8.0; GraphPad Software La Jolla, CA). Results were expressed as mean±SD. Significance ( $P<0.05$ ) between 2 groups was calculated using unpaired Student *t* test or paired *t* test after Shapiro-Wilks tests of normality

## RESULTS

### Ischemia Elicits Different CSDs and SHs Within the First Minutes

Thrombin injection led to a complete and rapid occlusion of the MCA, which caused a drop of perfusion in the cortical MCA territory to between 20% and 30% of baseline in the core region (Figure 1A and 1B, Figure S1).

In a first experiment, we used in vivo electrophysiology and laser speckle imaging simultaneously to assess both electrophysiological and hemodynamic characteristics of CSD after MCA occlusion ( $n=6$  mice). In general, CSD occurred spontaneously after stroke induction in all animals. CSD amplitude ( $13.04\pm 2.3$  mV), and duration (measured as full-width half-maximum:  $31.10\pm 5.2$  s) were consistent with prior descriptions of CSDs occurring during ischemia.<sup>31,32</sup> Analysis of the core and penumbral recordings revealed a spreading depolarization occurring massively in the penumbra compared to the core as evidenced by the characteristic propagating DC-potential shift (Figure 1C and 1D). Notably, when the DC trace showed a wave spreading dominantly in the penumbra, the hemodynamic recording showed SH response in the same region while a mild or no wave in the core was associated to no SH in the hemodynamic recording (Figures 1C and Video S1).

To understand the neurovascular responses to CSDs, we extracted hemodynamic signals by monitoring blood flow changes for 2 hours after MCA occlusion (Figure 2A and 2B). Therefore, in a second experiment, we identified SHs by their typical LSCI features: a steep transient increase in CBF followed by CBF recovery. SH occurred spontaneously after stroke induction in 12 out of 18 animals. Analysis of the core and penumbra areas revealed 2 different

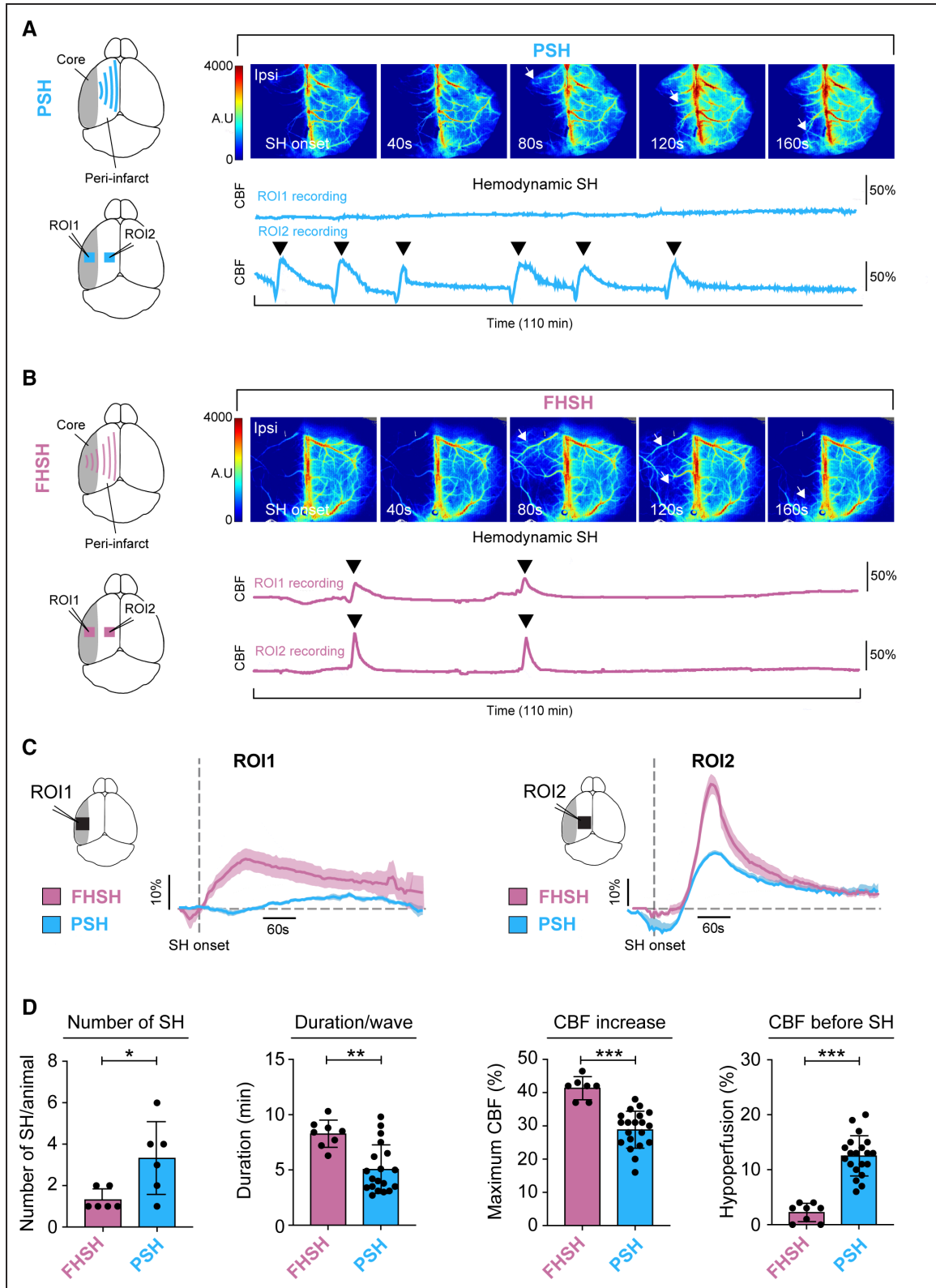


**Figure 2. Two patterns of spreading hyperemia (SH) in the thrombin model of stroke.**

Cerebral blood flow (CBF) recordings from penumbra spreading hyperemia (PSH) and full hemisphere spreading hyperemia (FHSH) mice. CBF was recorded in 2 different regions per animal: the core of the lesion (regions of interest [ROI1]) and the penumbra (ROI2). **A**, Schematic showing the spreading of PSH in ROI1 and ROI2 and representative laser speckle contrast imaging (LSCI) during a CSD onset in a PSH animal illustrating how SH wave propagates only through the penumbra (ROI2) after MCA occlusion. The color bar indicates perfusion in arbitrary units (A.U.). The graph shows representative recording of CBF changes from a PSH mouse (color-coded) acquired at 1 frame per second. There are no onsets of SHs that propagate in ROI1 while 6 onsets of SHs propagated in ROI2. **B**, Schematic showing the spreading of (Continued)

patterns of SH. In 6 animals, SH spread only through the penumbra area (Figure 2A and Video S1). In another 6, SH invaded the full ipsilateral hemisphere (Figure 2B and Video S1). In the last group of animals ( $n=6$ ), we observed no SHs at all during the 2 hours of CBF recording (Figure S2). Full hemisphere SHs were termed full hemisphere spreading hyperemia (FHSs) and penumbral SHs were termed penumbral spreading hyperemia (PSHs).

Notably, only one SH propagation pattern was observed in each of the affected animals. Furthermore, upon MCA occlusion no initial CBF differences between the 3 subgroups could be observed (Figure S1). Analysis of the contralateral side revealed a constant CBF during SH (Figure S3A). Additionally, in sham-operated mice ( $n=3$ ), no SH was detected (Figure S3B), confirming that SH was indeed due to stroke.

### FHSH and PSH Occur at Different Numbers, Amplitude, and Duration

We then compared the numbers and shapes of SH waves in ROI2 (penumbra area). We selected ROI2 because both FHSH and PSH groups showed SH in that area. In the FHSH group, the first SH occurred at a median of  $3.7 \pm 1.5$  minutes following MCA occlusion, while in the PSH group, the first SH occurred at a median  $6.7 \pm 3.9$  minutes. In the PSH group, the incidence of SHs was significantly higher compared to FHSH animals (Figure 2D). Furthermore, the duration of single PSHs were shorter than that of FHSHs ( $5.1 \pm 0.5$  minutes compared with  $8.3 \pm 0.4$  minutes; Figure 2D). The amplitude of the positive deflection of the SH wave was considerably larger in the FHSH ( $41.4 \pm 1.3\%$ ) compared with the PSH group ( $28.9 \pm 1.25\%$ ; Figure 2D). In terms of hypoperfusion before SH onset, the extent of the initial drop was larger in the PSH group ( $12.5 \pm 0.8\%$ ), while there was almost no hypoperfusion in the FHSH group ( $2.2 \pm 0.6\%$ ; Figure 2D).

### FHSH Is Associated With Smaller Lesion Size and Fewer Sensorimotor Deficits

After we found different patterns of SHs, we further tested whether the type of SH indicated the extent of tissue damage, hemorrhagic complications or functional outcome. Indeed, we observed significantly smaller infarct volumes in mice having FHSH ( $6.1 \pm 0.9 \text{ mm}^3$ ) compared with animals with PSH ( $21.6 \pm 2.8 \text{ mm}^3$ ; Figure 3A). Notably, lesion volumes in no-SH mice were intermediate

( $11.1 \pm 0.91 \text{ mm}^3$ ; Figure 3A). In line with these findings, hemorrhagic transformation occurred less often in FHSH animals (16.67%) and no-SH (33%) compared with PSH (100%; Figure 3A). While 80% of the PSH animals died during the 7 days of follow-up after stroke, there was no mortality in the FHSH or in the no-SH group. Neurological deficits were less severe in mice having FHSH, with significantly lower scores in the composite observational test on day 1 ( $10.3 \pm 0.61$  compared with  $8.8 \pm 0.48$ ) and day 3 ( $11 \pm 0.36$  compared with  $9.6 \pm 0.51$ ; Figures 3B). Furthermore, sensorimotor function assessed by the sticky tape test was better in FHSH compared to PSH mice (Figure 3C and 3D). In both tests, the no-SH group showed intermediate performance. We observed that higher amplitude and longer SH duration correlated with smaller infarcts and vice versa in PSH mice (Figure 3F).

### r-tPA Thrombolysis Decreases Lesion Volume and Improved Neurological Outcome in Both PSH and FHS

Thrombolysis with r-tPA has unequivocally been shown to improve outcome in ischemic stroke.<sup>33,34</sup> To investigate if targeting the hemodynamic responses to CSD impacts stroke outcome, mice were treated with r-tPA. r-tPA was infused in 21 mice showing PSH, FHSH or no SH. The occurrence of the PSH and FHSH throughout r-tPA infusion for up to 2 hours after ischemia is presented in Figures 4A and 4B. Interestingly, r-tPA infusion significantly modified the SH pattern in both PSH and FHSH groups. Indeed, wave duration in FHSH and PSH animals was reduced after r-tPA thrombolysis and hypoperfusion amplitude was reduced in PSH mice. Furthermore, we observed that r-tPA treatment, significantly reduced lesion volume compared with saline controls in both PSH and FHSH mice (Figure 4C and 4D). Overall r-tPA improved stroke outcome independent of SH pattern. Although, r-tPA did not significantly affect the hemorrhagic transformation and mortality rate, neurological score and sticky tape performance improved in the r-tPA treated mice in all groups (Figure 4C and 4D).

## DISCUSSION

We here show that the severity of tissue damage upon ischemia can be predicted by the type of hemodynamic response to CSD. We provide a better understanding of different SH propagation patterns after ischemia. Indeed,

**Figure 2 Continued.** FHSH in the core of lesion and the penumbra and representative LSCI recording during a CSD onset in a FHSH animal illustrating how the SH wave propagates through the whole hemisphere after MCA occlusion. The color bar indicates perfusion in arbitrary units (A.U.). The graph shows representative recordings of CBF changes in the ROIs from a FHSH mouse acquired at 1 frame per second. In the lower row, each black arrowheads indicate a singular SH. Note that there are 2 onsets of SH that propagate simultaneously in ROI1 and ROI2. Also note that each black arrow represents a singular SH. **C**, Averaged recordings of the ROI1 and ROI2 in FHSH and PSH animals. **D**, The number of SHs is lower in FHSH compared with PSH animals. The duration of SH waves is longer in the PSH group. The CBF response to SHs is smaller in PSH animals. The CBF reduction before each SH wave is higher in the PSH animals ( $n=6$  animals/group, \* $P<0.05$ ; \*\* $P<0.01$ ; \*\*\* $P<0.001$ ; Mann-Whitney  $U$  test).

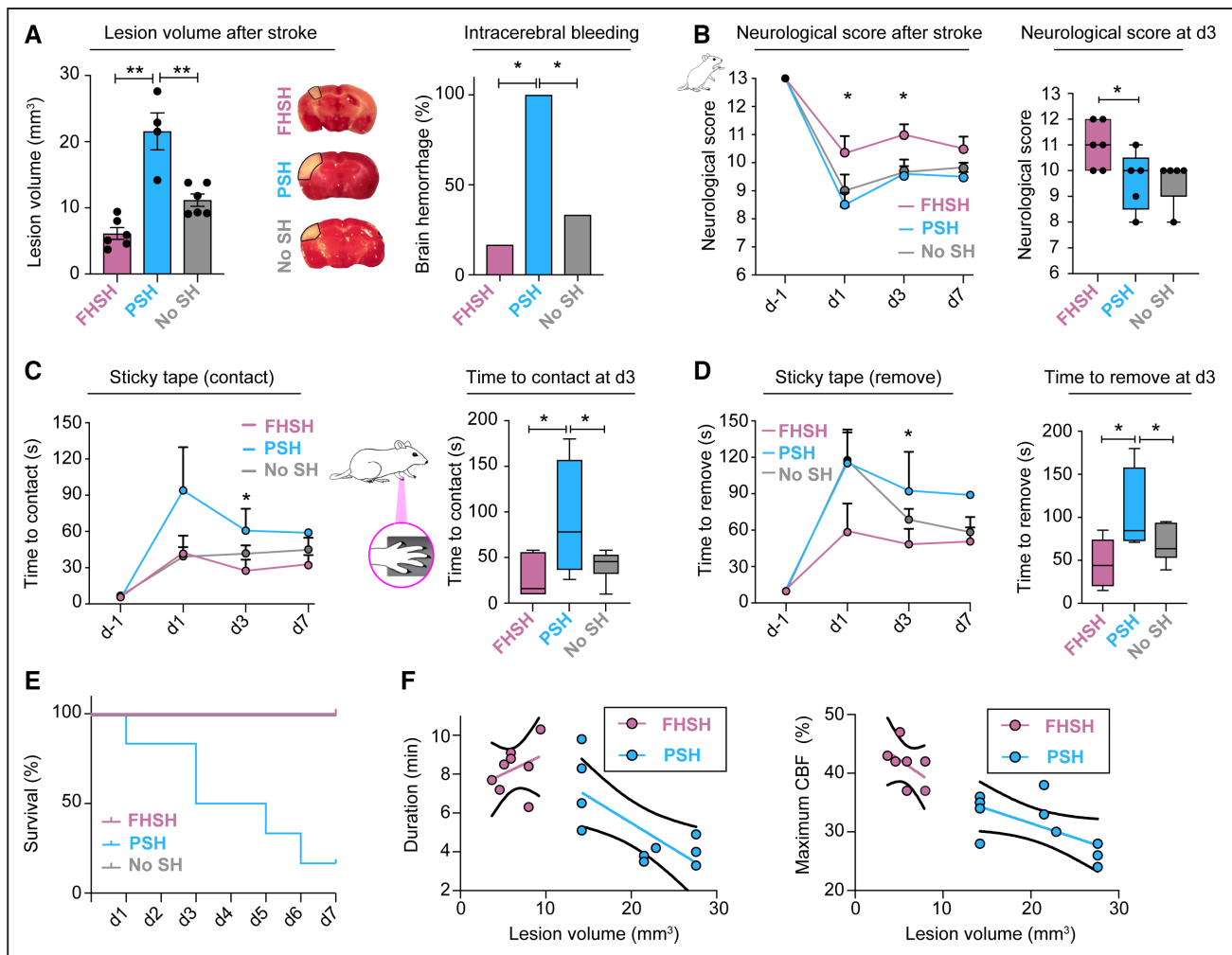


**Figure 3. Lesion volume and sensorimotor deficits in animals according to spreading hyperemia (SH) type.**

**A**, Three representative 2,3-triphenyltetrazolium chloride (TTC)-stained brain sections showing lesions (pale) in each group. Bar graph depicting infarct volumes from individual full hemisphere spreading hyperemia (FHSH), penumbral spreading hyperemia (PSH), and no-SH mice (n=6 animals/group). On the **right**, fraction of mice with intracerebral hemorrhage detected on TTC-stains after stroke in FHSH, PSH and no-SH groups. **B–D**, Neurological score and sticky tape removal assessment in FHSH, PSH, and no-SH mice at days 1, 3, and 7 after stroke. **E**, Overall survival rate in the 3 groups. **F**, Duration and amplitude of SHs correlated with lesion volumes. \* $P < 0.05$ , \*\* $P < 0.01$ , 1-way Kruskal-Wallis ANOVA with post hoc Dunn multiple-comparison correction to compare between groups. Data are mean  $\pm$  SD.

from the first minutes after MCA occlusion, the cortex experienced spontaneous SH. When confined only to penumbra areas, PSHs were associated with deleterious effects and progressive tissue damage. On the contrary, FHSHs were associated with a beneficial infarct outcome and a potential viability of the infarct core. Moreover, independent of SH pattern, thrombolysis improved stroke outcome, further reducing lesion volume and neurological deficits. Interestingly, upon r-tPA thrombolysis, the occurrence of SHs did not change, however, their features such as duration of the wave and hypoperfusion amplitude was significantly reduced. The difference in outcome could not be explained by a more severe initial drop of perfusion after ischemia. Therefore, the type of SH informed early about prognosis as well as response to thrombolysis. In this study, we report the existence of beneficial SHs post ischemia. Furthermore, our data

show that targeting the hemodynamic alterations due to CSD is a promising strategy for stroke treatment.

We could demonstrate by simultaneously measuring electrophysiological changes and hemodynamic responses that the timing as well as the propagation of SHs was generated by spreading depolarization.

One of the early features of stroke is the disruption of neuronal activity resulting from the reduction of metabolic supply.<sup>35</sup> Increased electrical activity causes glutamate evoked calcium influx in postsynaptic neurons, activating the release of vasodilating factors, such as nitric oxide and arachidonic acid metabolites, which increase local CBF.<sup>9</sup> When CSD occurs, the most typical hemodynamic response is a propagating SH wave as a result of local vasodilation. One unsolved question is whether the CBF responses indicate expansion of the ischemic territory. To address this question, we used real-time LSCI, a minimally



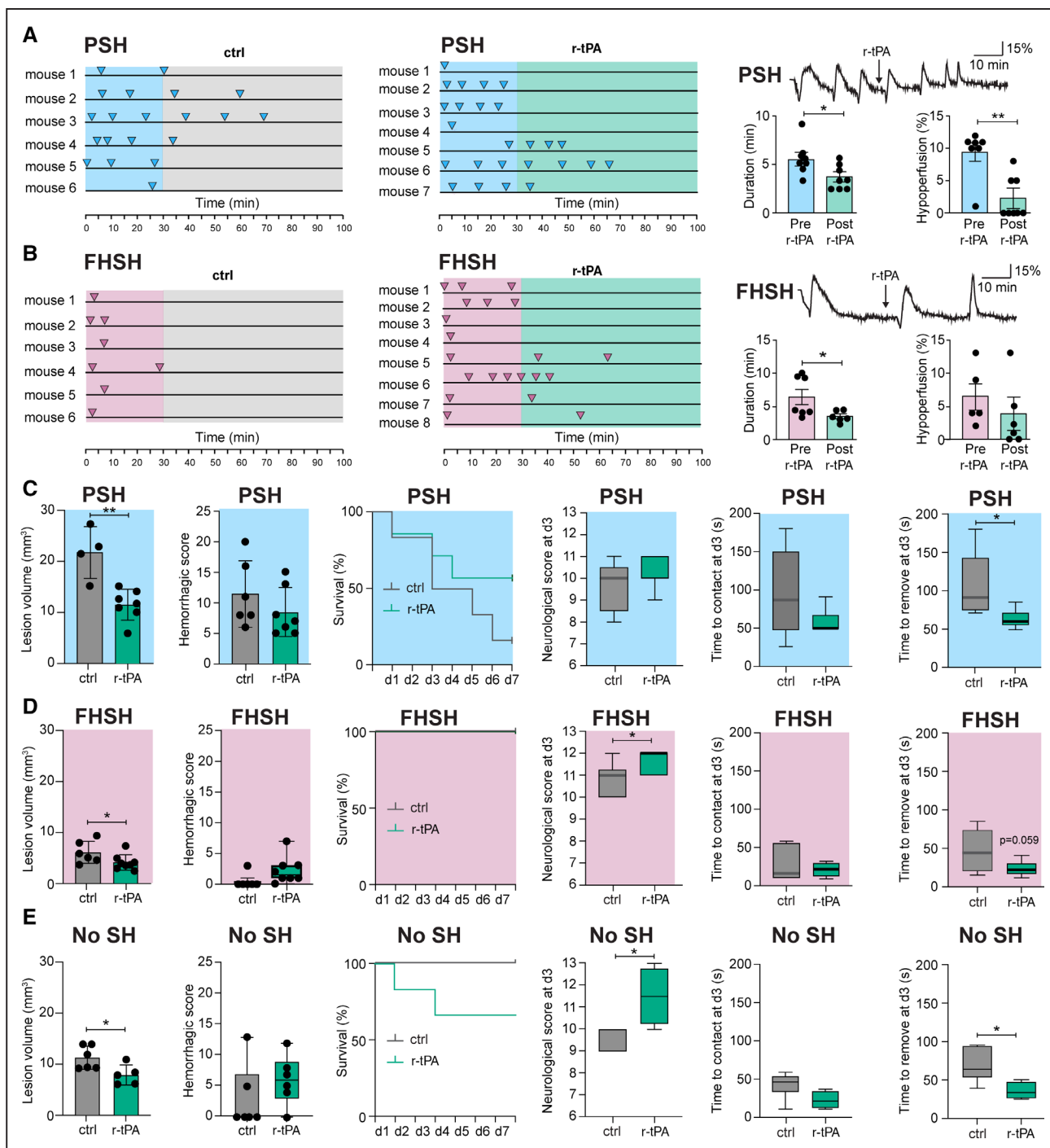


**Figure 4. Spreading hyperemia waves after ischemia and thrombolysis with r-tPA (recombinant tissue-type plasminogen activator).**

**A** and **B**. Each line represents an animal/experiment and each arrow represents a singular spreading hyperemia (SH). Representative recording pre- and post r-tPA for penumbral spreading hyperemia (PSH) and full hemisphere spreading hyperemia (FHS) animals. r-tPA significantly reduced duration of FHSs and PSHs and the amplitude of hypoperfusions in PSH animals. **C–E**. Treatment with r-tPA attenuated the deleterious tissue and neurological outcome associated with PSH, FHS, and no SH mice (n=6–8 mice/group). Bar graphs representing lesion volume, hemorrhagic score and survival rate in r-tPA compared with control treated PSH, FHS, and no SH animals. Neurological score and sticky tape removal assessment in FHS, PSH, and no-SH mice at day 3 after r-tPA treatment compared with control (\**P*<0.05; \*\**P*<0.01; Mann–Whitney *U* test).

invasive imaging tool to monitor CBF changes throughout the whole cortex.<sup>21</sup> LSCI revealed that the pattern of SH predicted the severity of stroke and response to treatment. As previously described in the literature, the more affected the tissue, the stronger the hypoperfusion response, and

the more severe the loss of perfusion.<sup>36</sup> Heterogeneity in SH propagation may depend on differences in intrinsic excitability across the ischemic tissue, or on neurovascular decoupling. In animals with PSH, the core was not showing any SH response, suggesting that either CSDs do not

propagate because of severe neuronal damage or that the hemodynamic and electrical responses are decoupled due to severe vascular damage. PSHs began with a brief negative deflection of the CBF curve (hypoperfusion response), resulting in expansion of the ischemic core, which is in line with observations made in penumbral spreading depolarizations.<sup>6</sup> Strikingly, our data showed another pattern of SH propagation across the infarct core in FHS. The demonstration of FHS introduces the novel concept of a SH that does not reflect lesion growth, but on the contrary, tissue viability. We hypothesize that FHSs are a biological marker of a restorative vascular response that indicates potential tissue recovery. This suggests that cortical tissue in the infarct core is still at least partially viable, because necrotic tissue would be unable to generate SH. Such transient hyperemic flow patterns in the whole hemisphere could be protective by alleviating tissue acidosis as previously found in a model of focal ischemia due to brain topical application of the vasoconstrictor endothelin-1.<sup>37</sup> Indeed, the transient increase of whole hemisphere CBF in the FHS group may booster hemodynamic forces evoking reperfusion. Interestingly, our hypothesis is supported by the fact that the no-SH group showed intermediate effects in tissue injury and neurological outcome. Compared with other stroke models, using predominantly intraluminal MCA occlusion models,<sup>6,38,39</sup> the thromboembolic stroke model did not induce inverted hemodynamic responses to spreading depolarizations.

The area we defined as an ischemic penumbra corresponds to the outer penumbra described in the continuum of spreading depolarizations with 55% of residual CBF.<sup>5</sup> Using intravital 2-photon microscopy, we have previously shown that this region shows dynamic alteration on the microvascular level.<sup>21</sup> Today, it is widely accepted that the discrimination between penumbra and core is challenging and that there is considerable variability of CBF thresholds to define these regions.<sup>40</sup> These depend on the methods used for flow determination, the different species, different stroke models, the time of measurement after ischemia, and whether occlusion was permanent or temporary. As an alternative to this hemodynamic concept, additional studies could include combined MR perfusion-weighted imaging and MR diffusion-weighted imaging.

Current imaging biomarkers of stroke outcome have to be related to reperfusion therapy, since this is the mainstay of stroke treatment in the clinic.<sup>35,41</sup> We found that thrombolysis with r-tPA result in smaller lesion volumes and less neurological deficits independent of SH pattern. We focused on the hemodynamic response of CSDs, because this provides the most accessible mean to study SH non-invasively in the whole mouse brain. The observed SH patterns could be a useful biomarker for stroke severity.

The acute phase after the onset of ischemia is a crucial time window for treatment. Thrombolysis with r-tPA is not always beneficial, and depending on time and individual factors, the risk of hemorrhagic complications might be

high.<sup>30,41,42</sup> There is an urgent need to develop reliable biomarkers to help decision-making in patients with stroke. Transient SHs are an example of early, dynamic blood flow changes that could be adapted as clinical imaging read-outs of stroke severity and treatment efficacy.

Furthermore, our observations could guide future work aiming to determine how different kinds of CSD and their hemodynamic response might affect outcomes following stroke, and how this could be modified to the benefit of patients with stroke.

## ARTICLE INFORMATION

Received May 12, 2021; final revision received December 24, 2021; accepted February 1, 2022.

### Affiliations

Department of Neurology, University Hospital Zurich and University of Zurich (UZH), Switzerland (N.F.B., W.M., N.P., S.W., M.E.A.). Institute of Pharmacology and Toxicology, Experimental Imaging and Neuroenergetics, University of Zurich (UZH), Switzerland (C.G., M.T.W., B.W.). Neuroscience Center Zurich (ZNZ), University of Zurich and ETH Zurich, Switzerland (N.F.B., C.G., W.M., N.P., B.W., S.W., M.E.A.). Normandie University, Unirouen, INSERM U1239, Rouen, France (M.A., J.C.). Normandie University, Unirouen, IRIB, EA3830-GRHVN, Rouen, France (J.C.).

### Acknowledgments

All study data are included in the article. Author contributions: Dr Amki, Dr Binder, Dr Chuquet and M. Alasoadura performed research. Dr Binder, M. Alasoadura, and W. Middleham analyzed data. Dr Amki, Dr Chuquet and Dr Wegener designed research. Dr Weber, Dr Wegener, and Dr Amki supervised the project. Drs Amki, Weber and Wegener acquired the funding and reviewed the article. Dr Binder, Dr Glück, Dr Wyss, and W. Middleham wrote the article.

### Sources of Funding

This study was supported by the Swiss National Science Foundation (SNSF) PP00P3\_170683, the Swiss Heart Foundation and the University of Zurich Clinical Research Priority Program (CRPP) Stroke.

### Disclosures

None.

### Supplemental Material

Figures S1–S3  
Video S1

## REFERENCES

1. Ka H. Perinfarct depolarizations. *Cerebrovasc Brain Metab Rev*. 1996;8:195–208.
2. Ayata C, Lauritzen M. Spreading depression, spreading depolarizations, and the cerebral vasculature. *Physiol Rev*. 2015;95:953–993. doi: 10.1152/physrev.00027.2014
3. Schoknecht K, Kikhia M, Lemale CL, Liotta A, Lublinsky S, Mueller S, Boehm-Sturm P, Friedman A, Dreier JP. The role of spreading depolarizations and electrographic seizures in early injury progression of the rat photothrombosis stroke model. *J Cereb Blood Flow Metab*. 2021;41:413–430. doi: 10.1177/0271678X20915801
4. Dreier JP, Reiffurth C. The stroke-migraine depolarization continuum. *Neuron*. 2015;86:902–922. doi: 10.1016/j.neuron.2015.04.004
5. Hartings JA, Shuttleworth CW, Kirov SA, Ayata C, Hinzman JM, Foreman B, Andrew RD, Boutelle MG, Brennan KC, Carlson AP, et al. The continuum of spreading depolarizations in acute cortical lesion development: examining Leão's legacy. *J Cereb Blood Flow Metab*. 2017;37:1571–1594. doi: 10.1177/0271678X16654495
6. Shin HK, Dunn AK, Jones PB, Boas DA, Moskowitz MA, Ayata C. Vasoconstrictive neurovascular coupling during focal ischemic depolarizations. *J Cereb Blood Flow Metab*. 2006;26:1018–1030. doi: 10.1038/sj.jcbfm.9600252
7. Dohmen C, Sakowitz OW, Fabricius M, Bosche B, Reithmeier T, Ernestus RI, Brinker G, Dreier JP, Woitzik J, Strong AJ, et al; Co-Operative Study of

- Brain Injury Depolarisations (COSBID). Spreading depolarizations occur in human ischemic stroke with high incidence. *Ann Neurol*. 2008;63:720–728. doi: 10.1002/ana.21390
8. Dreier JP. The role of spreading depression, spreading depolarization and spreading ischemia in neurological disease. *Nat Med*. 2011;17:439–447. doi: 10.1038/nm.2333
  9. Taş YÇ, Sularoğlu İ, Gürsoy-Özdemir Y. Spreading depolarization waves in neurological diseases: a short review about its pathophysiology and clinical relevance. *Curr Neuropharmacol*. 2019;17:151–164. doi: 10.2174/1570159X15666170915160707
  10. Strong K, Mathers C, Bonita R. Preventing stroke: saving lives around the world. *Lancet Neurol*. 2007;6:182–187. doi: 10.1016/S1474-4422(07)70031-5
  11. Lückl J, Lemale CL, Kola V, Horst V, Khojasteh U, Oliveira-Ferreira AI, Major S, Winkler MKL, Kang EJ, Schoknecht K, et al. The negative ultraslow potential, electrophysiological correlate of infarction in the human cortex. *Brain*. 2018;141:1734–1752. doi: 10.1093/brain/awy102
  12. Dreier JP, Ebert N, Priller J, Megow D, Lindauer U, Klee R, Reuter U, Imai Y, Einhüpl KM, Victorov I, et al. Products of hemolysis in the subarachnoid space inducing spreading ischemia in the cortex and focal necrosis in rats: a model for delayed ischemic neurological deficits after subarachnoid hemorrhage? *J Neurosurg*. 2000;93:658–666. doi: 10.3171/jns.2000.93.4.0658
  13. Dreier JP, Körner K, Ebert N, Görner A, Rubin I, Back T, Lindauer U, Wolf T, Villringer A, Einhüpl KM, et al. Nitric oxide scavenging by hemoglobin or nitric oxide synthase inhibition by N-nitro-L-arginine induces cortical spreading ischemia when K<sup>+</sup> is increased in the subarachnoid space. *J Cereb Blood Flow Metab*. 1998;18:978–990. doi: 10.1097/00004647-199809000-00007
  14. Mies G, Iijima T, Hossman KA. Correlation between peri-infarct DC shifts and ischaemic neuronal damage in rat. *Neuroreport*. 1993;4:709–711. doi: 10.1097/00001756-199306000-00027
  15. Seidel JL, Escartin C, Ayata C, Bonvento G, Shuttleworth CW. Multifaceted roles for astrocytes in spreading depolarization: A target for limiting spreading depolarization in acute brain injury? *Glia*. 2016;64:5–20. doi: 10.1002/glia.22824
  16. Nakamura H, Strong AJ, Dohmen C, Sakowitz OW, Vollmar S, Sué M, Kracht L, Hashemi P, Bhatia R, Yoshimine T, et al. Spreading depolarizations cycle around and enlarge focal ischaemic brain lesions. *Brain*. 2010;133(pt 7):1994–2006. doi: 10.1093/brain/awq117
  17. Kirov SA, Fomitcheva IV, Sword J. Rapid neuronal ultrastructure disruption and recovery during spreading depolarization-induced cytotoxic edema. *Cereb Cortex*. 2020;30:5517–5531. doi: 10.1093/cercor/bhaa134
  18. Dreier JP, Lemale CL, Kola V, Friedman A, Schoknecht K. Spreading depolarization is not an epiphenomenon but the principal mechanism of the cytotoxic edema in various gray matter structures of the brain during stroke. *Neuropharmacology*. 2018;134(Pt B):189–207. doi: 10.1016/j.neuropharm.2017.09.027
  19. Sueiras M, Thonon V, Santamarina E, Sánchez-Guerrero Á, Riveiro M, Poca MA, Quintana M, Gándara D, Sahuquillo J. Is Spreading depolarization a risk factor for late epilepsy? A prospective study in patients with traumatic brain injury and malignant ischemic stroke undergoing decompressive craniectomy. *Neurocrit Care*. 2021;34:876–888. doi: 10.1007/s12028-020-01107-x
  20. Woitzik J, Hecht N, Pinczolis A, Sandow N, Major S, Winkler MK, Weber-Carstens S, Dohmen C, Graf R, Strong AJ, et al; COSBID study group. Propagation of cortical spreading depolarization in the human cortex after malignant stroke. *Neurology*. 2013;80:1095–1102. doi: 10.1212/WNL.0b013e3182886932
  21. El Amki M, Glück C, Binder N, Middleham W, Wyss MT, Weiss T, Meister H, Luft A, Weller M, Weber B, et al. Neutrophils obstructing brain capillaries are a major cause of no-reflow in ischemic stroke. *Cell Rep*. 2020;33:108260. doi: 10.1016/j.celrep.2020.108260
  22. Orset C, Macrez R, Young AR, Panthou D, Angles-Cano E, Maubert E, Agin V, Vivien D. Mouse model of in situ thromboembolic stroke and reperfusion. *Stroke*. 2007;38:2771–2778. doi: 10.1161/STROKEAHA.107.487520
  23. El Amki M, Lerouet D, Coqueran B, Curis E, Orset C, Vivien D, Plotkine M, Marchand-Leroux C, Margail I. Experimental modeling of recombinant tissue plasminogen activator effects after ischemic stroke. *Exp Neurol*. 2012;238:138–144. doi: 10.1016/j.expneurol.2012.08.005
  24. Dreier JP, Fabricius M, Ayata C, Sakowitz OW, Shuttleworth CW, Dohmen C, Graf R, Vajkoczy P, Helbok R, Suzuki M, et al. Recording, analysis, and interpretation of spreading depolarizations in neurointensive care: review and recommendations of the COSBID research group. *J Cereb Blood Flow Metab*. 2017;37:1595–1625. doi: 10.1177/0271678X16654496
  25. Baumgartner P, El Amki M, Bracko O, Luft AR, Wegener S. Sensorimotor stroke alters hippocampo-thalamic network activity. *Sci Rep*. 2018;8:15770. doi: 10.1038/s41598-018-34002-9
  26. Prestigiacomo CJ, Kim SC, Connolly ES Jr, Liao H, Yan SF, Pinsky DJ. CD18-mediated neutrophil recruitment contributes to the pathogenesis of reperfusion but not nonreperfusion stroke. *Stroke*. 1999;30:1110–1117. doi: 10.1161/01.str.30.5.1110
  27. David HN, Haelewyn B, Rizzo JJ, Colloc'h N, Abraini JH. Xenon is an inhibitor of tissue-plasminogen activator: adverse and beneficial effects in a rat model of thromboembolic stroke. *J Cereb Blood Flow Metab*. 2010;30:718–728. doi: 10.1038/jcbfm.2009.275
  28. El Amki M, Binder N, Steffen R, Schneider H, Luft AR, Weller M, Imthurn B, Merki-Feld GS, Wegener S. Contraceptive drugs mitigate experimental stroke-induced brain injury. *Cardiovasc Res*. 2019;115:637–646. doi: 10.1093/cvr/cvy248
  29. Bouet V, Boulouard M, Toutain J, Divoux D, Bernaudin M, Schumann-Bard P, Freret T. The adhesive removal test: a sensitive method to assess sensorimotor deficits in mice. *Nat Protoc*. 2009;4:1560–1564. doi: 10.1038/nprot.2009.125
  30. El Amki M, Lerouet D, Garraud M, Teng F, Beray-Berthet V, Coqueran B, Barsacq B, Abbou C, Palmier B, Marchand-Leroux C, et al. Improved reperfusion and vasculoprotection by the Poly(ADP-Ribose)polymerase inhibitor PJ34 after stroke and thrombolysis in mice. *Mol Neurobiol*. 2018;55:9156–9168. doi: 10.1007/s12035-018-1063-3
  31. Lauritzen M, Dreier JP, Fabricius M, Hartings JA, Graf R, Strong AJ. Clinical relevance of cortical spreading depression in neurological disorders: migraine, malignant stroke, subarachnoid and intracranial hemorrhage, and traumatic brain injury. *J Cereb Blood Flow Metab*. 2011;31:17–35. doi: 10.1038/jcbfm.2010.191
  32. Farkas E, Bari F, Obrenovitch TP. Multi-modal imaging of anoxic depolarization and hemodynamic changes induced by cardiac arrest in the rat cerebral cortex. *Neuroimage*. 2010;51:734–742. doi: 10.1016/j.neuroimage.2010.02.055
  33. Neuhaus AA, Couch Y, Hadley G, Buchan AM. Neuroprotection in stroke: the importance of collaboration and reproducibility. *Brain*. 2017;140:2079–2092. doi: 10.1093/brain/awx126
  34. Zerna C, Thomalla G, Campbell BCV, Rha JH, Hill MD. Current practice and future directions in the diagnosis and acute treatment of ischaemic stroke. *Lancet*. 2018;392:1247–1256. doi: 10.1016/S0140-6736(18)31874-9
  35. Campbell BCV, De Silva DA, Macleod MR, Coutts SB, Schwamm LH, Davis SM, Donnan GA. Ischaemic stroke. *Nat Rev Dis Primers*. 2019;5:70. doi: 10.1038/s41572-019-0118-8
  36. Bere Z, Obrenovitch TP, Kozák G, Bari F, Farkas E. Imaging reveals the focal area of spreading depolarizations and a variety of hemodynamic responses in a rat microembolic stroke model. *J Cereb Blood Flow Metab*. 2014;34:1695–1705. doi: 10.1038/jcbfm.2014.136
  37. Oliveira-Ferreira AI, Milakara D, Alam M, Jorks D, Major S, Hartings JA, Lückl J, Martus P, Graf R, Dohmen C, et al; COSBID study group. Experimental and preliminary clinical evidence of an ischemic zone with prolonged negative DC shifts surrounded by a normally perfused tissue belt with persistent electrocorticographic depression. *J Cereb Blood Flow Metab*. 2010;30:1504–1519. doi: 10.1038/jcbfm.2010.40
  38. Feuerstein D, Takagaki M, Gramer M, Manning A, Endepols H, Vollmar S, Yoshimine T, Strong AJ, Graf R, Backes H. Detecting tissue deterioration after brain injury: regional blood flow level versus capacity to raise blood flow. *J Cereb Blood Flow Metab*. 2014;34:1117–1127. doi: 10.1038/jcbfm.2014.53
  39. Strong AJ, Anderson PJ, Watts HR, Virley DJ, Lloyd A, Irving EA, Nagafuji T, Ninomiya M, Nakamura H, Dunn AK, et al. Peri-infarct depolarizations lead to loss of perfusion in ischaemic gyrencephalic cerebral cortex. *Brain*. 2007;130(pt 4):995–1008. doi: 10.1093/brain/awl392
  40. del Zoppo GJ, Sharp FR, Heiss WD, Albers GW. Heterogeneity in the penumbra. *J Cereb Blood Flow Metab*. 2011;31:1836–1851. doi: 10.1038/jcbfm.2011.93
  41. El Amki M, Wegener S. Improving cerebral blood flow after arterial recanalization: a novel therapeutic strategy in stroke. *Int J Mol Sci*. 2017;18:E2669. doi: 10.3390/ijms18122669
  42. Whiteley WN, Emberson J, Lees KR, Blackwell L, Major G, Bluhmki E, Brott T, Cohen G, Davis S, Donnan G, et al; Stroke Thrombolysis Trialists' Collaboration. Risk of intracerebral haemorrhage with alteplase after acute ischaemic stroke: a secondary analysis of an individual patient data meta-analysis. *Lancet Neurol*. 2016;15:925–933. doi: 10.1016/S1474-4422(16)30076-X